Pirot and Omer
Journal of Analytical Science and Technology (2022) 13:22
https://doi.org/10.1186/s40543-022-00333-6

Journal of Analytical Science and Technology

RESEARCH ARTICLE

Open Access

Designing of robust and sensitive assay via encapsulation of highly emissive and stable blue copper nanocluster into zeolitic imidazole framework (ZIF-8) with quantitative detection of tetracycline

Shano M. Pirot and Khalid M. Omer*

Abstract

Metal–organic frameworks (MOFs) with high stability and porosity have gained great attention in bioanalysis due to their potential in improving sensitivity and robustness of assays. Herein, to improve both the stability and the emission intensity of Cu nanoclusters (CuNCs), in situ entrapment strategy of CuNCs into zeolitic imidazolate framework-8 (ZIF-8) is described. Blue emissive and stable CuNCs was prepared, for the first time, using thiamine hydrochloride as capping agents, and showed strong and stable emission at 440 nm when excited at 375 nm with fluorescence quantum yields 12%. Encapsulation of CuNC into ZIF-8 showed dramatic enhancement of the fluorescence intensity up to 53% fluorescence quantum yield. Furthermore, the CuNCs@ZIF-8 possesses better stability (more than three months) due to protective and confinement effect of MOFs. Upon the addition of tetracycline to CuNCs@ZIF-8 solution, the blue emission intensity was significantly decreased. The fluorescence ratio (Fo/F) against the concentration of tetracycline exhibited a satisfactory linear relationship from 1.0 to 10.0 μM with a detection limit (LOD) of 0.30 μM. The current probe was applied for quantification of tetracycline in drug sample with satisfactory accuracy and precision.

Keywords: Copper nanoclusters, Zeolitic imidazole framework, ZIF-8, MOF, Tetracycline

*Correspondence: khalid.omer@univsul.edu.iq

Center for Biomedical Analysis, Department of Chemistry, College of Science, University of Sulaimani, Qliasan St, 46002 Sulaimani City, Kurdistan Region, Iraq

Graphical abstract

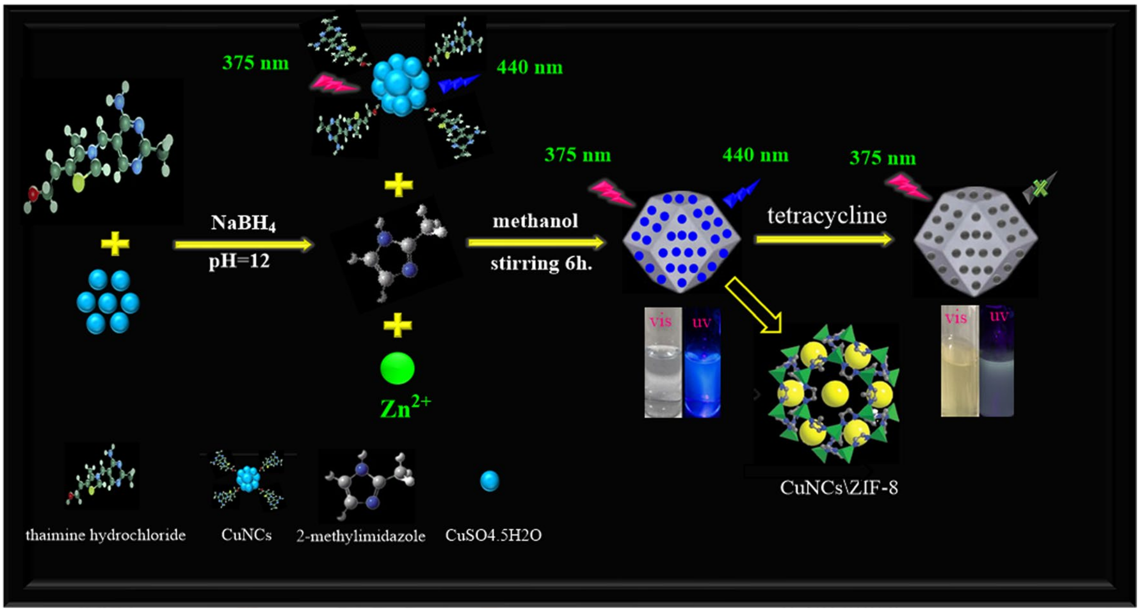

Introduction

Robustness and sensitivity are two important criteria in figures of merits of a particular bioassay. Based on the common definition, robustness is a capacity of an analytical procedure to produce unbiased results in the presence of small changes in the test conditions. Hence, one should think about methods and approaches to improve robustness of a bioanalytical method.

Metal–organic frameworks (MOFs) gain more interests for a decade in biochemical sensing applications. MOFs are crystalline porous compounds contain a metal ion or cluster connected by organic ligands to form one, two, or three-dimensional infinite networks (Yaghi et al. 1995; Bågenholm et al. 1996; Sutrisna et al. 2020; Troyano et al. 2019; Doonan et al. 2017; Kreno et al. 2012; Li et al. 1999). MOFs have many unique properties including high thermal stability, variable pore sizes, high surface area, structural diversity, and tunable shapes (Jalili et al. 2019; Han et al. 2015; Bazargan et al. 2021). Thus, MOFs are employed in various fields such as catalysis (Li et al. 2018a; Bin et al. 2020; Zhang et al. 2013; Wei et al. 2020), sensing (Online et al. 2014; Wu et al. 2017; Shahat et al. 2013; Kumar et al. 2015), adsorbent (Qu et al. 2017; Liu et al. 2014; Rowsell et al. 2005; Düren and Snurr 2004; Li et al. 2009), drug transportation (Sun et al. 2017a; Wan et al. 2019; Liu et al. 2016,) and energy (Sun et al. 2017b; So et al. 2015; Wang et al. 2017a; Baumann et al. 2019).

In recent years, a number of reports have been published on the investigating and using of MOFs in biochemical sensing via preparation and functionalization of various types of MOFs (Cui et al. 2016; Koo et al. 2019). One of the classes that is used in biochemical sensing is luminescent MOFs (LMOFs). The MOFs might have own intrinsic luminescence property or might be functionalized to show luminescence (Müller-Buschbaum et al. 2015; Allendorf et al. 2009; Zhang et al. 2018; Cui et al. 2012). In other words, one can add luminescent materials into the non-luminescent MOFs to produce functionalized LMOFs. For instance, Buso et al. (Buso et al. 2012) synthesized LMOFs by insertion fluorescent quantum dots (QDs) after appropriate surface functionalization within MOF-5 crystals. MOF-5 (also known as IRMOF-1) is one of the most typical representatives of the MOFs family. It is a three-dimensional framework structure composed of terephthalic acid and metal cluster Zn_4O, firstly synthesized by Yaghi et al. (Li et al.1999) The QDs are solubilized within MOF-5 growth media; hence, it permits the incorporation of the QDs within the evolving framework during the reaction. Hao et al. (2017) synthesized a nanocomposite form fluorescent carbon dots (CDs) in Eu-2,6-pyridinedicarboxylic acid metal organic frameworks (Eu-DPA-MOFs) for the detection of Cu^{2+}. The CDs@Eu-DPA MOFs exhibited the uniform ball-flower-like nanostructures and were very stable in aqueous solution due to their nanoscale size and the ball-flower-like nanostructures. The porous nanostructures could also provide a large specific surface to increase the contact area between the probe and Cu^{2+}, which improved the sensitivity of the sensor.

In 2002, Yaghi et al (2003) discovered a new class of the MOF family which they introduced as zeolitic imidazolate frameworks (ZIFs). Compared to other MOFs, ZIFs displayed excellent photochemical, thermal, and chemical stability (Park et al. 2006). The repeating unit of Si–O–Si in zeolites is represented in ZIFs, with imidazolates in place of the bridging O atoms and transition metals (M) in place of the Si atoms. The angle made by M-IM-O is 145°, the same as that of Si–O–Si (Gao et al. 2009; Lewis et al. 2009; Ghaee et al. 2019; Shah et al. 2012).

In literature, a number of ZIFs have been prepared and coded as well-form ZIF-1 to ZIF-100, such as ZIF-8, ZIF-11, ZIF 67, and ZIF-69 (Shah et al. 2012; Noh et al. 2018). ZIF-8, which is one of the common ones, prepared from Zn^{2+} ions and 2-methylimidazole. ZIF-8 is a famous ZIF amongst nano/microporous MOFs due to its large surface area (about 1700 m^2/g), easy preparation, high thermal stability (400 °C), highly porous structure, and low density (Kolmykov et al. 2017; Taheri et al. 2021; Wang et al. 2017b; Hoseinpour and Shariatinia 2021; Lee et al. 2015). The topology of ZIF-8 corresponds to the zeolite sodalite, which can be described as a space-filling packing of truncated octahedrons (Hoseinpour and Shariatinia 2021; Hu et al. 2011; Lai 2018).

Up to now, different nanoparticles and fluorophores, such as fluorescent dyes (Chin et al. 2018; Liu et al. 2019; Han et al. 2016; Wang et al. 2018; Jing et al. 2014; Chandra and Nath 2020; Hu et al. 2018a), carbon nanomaterials (Wang et al. 2019; Li et al. 2018b; Wei et al. 2019; Wang et al. 2021), and quantum dots, have been used for biochemical sensing. (Omer and Hassan 2017; Omer and Sartin 2019; Omer et al. 2020; Mohammed and Omer 2020; Omer et al. 2020) However, due to aggregation-induced quenching, they suffer from diminishing their luminescence efficiency. MOFs give this porous platform to spread and stabilize those luminescent materials. The aforementioned luminescent materials were encapsulated successfully into MOF moieties (Chen et al. 2018a; Majewski et al. 2017; Chen et al. 2017a).

For example, Jalili prepared a dual-emissive metal–organic frameworks by encapsulating yellow-emitting and blue-emitting carbon dots into the zeolitic imidazolate framework (BYCDs@ZIF-8) which acted as a ratiometric probe for glutathione (Li et al. 2018b). Metal nanoclusters AuNCs, AgNCs, and CuNCs are widely prepared and used in various applications because of having excellent features including high fluorescence, excellent resistance to photobleaching, and biocompatibility compared with organic dyes and toxic quantum dots, large stokes shifts, low toxicity, and unique size-dependent fluorescence properties (Wang et al. 2017c). The most important reasons for using CuNCs are because of their good optical properties, low cost, abundance, and readily available element (Lin et al. 2021). Yang et al. prepared a highly fluorescent Cu nanocluster using L-cysteine as the stabilizer and then using the clusters for detection Hg^{2+} in a urine sample (Chen et al. 2017b). Most of the current approaches for increasing the fluorescence intensity of metal NCs are depend on strategies such as aggregation-induced emission (AIE) (Hu et al. 2018b), restriction of intramolecular motion (RIM) (Tian et al. 2015), and crystallization (Chen et al. 2017b).

Tetracycline (TC) displays antimicrobial activity against a wide range of gram-positive and gram-negative bacteria that was discovered in the mid-1900s (Conzuelo et al. 2012; Fahelelbom 2008). The low-cost antibacterials are among the most often used antibiotics, both in human medicine for the treatment of infectious illnesses and in the livestock sector as preventative and curative medications. They are also used as animal feed additives to stimulate quick animal development and weight increase (Spisso et al. 2007). On the other hand, TC is difficult for organisms to totally breakdown, and long-term exposure to it can promote drug resistance genes, lower the body's immunity to numerous illnesses, and even cause endocrine disorder in organism (Chopra and Roberts 2001; Sarmah et al. 2006).

Several analytical methods were used for determination of TC in pharmaceutical formulations including chemiluminescence (Han and He 1999), high-performance liquid chromatography (HPLC) (Wang et al. 2008), surface plasmon resonance spectroscopy (Ben-Amram et al. 2010), electrochemical immunosensors (Conzuelo et al. 2012), liquid chromatography (Aga et al. 2005), enzyme-linked immunoassay (Jeon et al. 2008), and voltammetric analysis (Ni et al. 2011). Shen et al. determined tetracycline using colorimetric assay utilizing the formation of gold nanoparticles in fluidic sample (Shen et al. 2014). The abovementioned methods, some of them, suffer from costly instrumentations and personnel skill, and some suffer from high LOD and instability of the probe. Thus, sensitive, selective, and stable probe is highly desirable for detection of TC in various matrices.

In this work, a nanocomposite is prepared via encapsulating of CuNCs into ZIF-8 nanostructure which is selective and sensitive for the trace level detection of TC in pharmaceutical formulations. CuNCs were prepared using thiamine hydrochloride as a stabilizing agent, for the first time, and $NaBH_4$ as a reducing agent to produce stable and highly emissive blue emission peak at 440 nm.

Interestingly, compared with the CuNCs, the CuNCs@ZIF-8 composites display stronger stability and more sensitivity for detecting TC. This makes CuNCs@ZIF-8 a unique and desirable probe to detect TC content in drug samples. Figure 1 shows the scheme for preparation of the nanocomposite and detection of tetracycline.

Experimental

Chemicals and reagents

All the reagents used were of analytical grade purchased from commercial suppliers (Merck and Sigma-Aldrich) and were used without further purification. Thiamine hydrochloride, sodium borohydride ($NaBH_4$), sodium hydroxide (NaOH), copper sulfate pentahydrate ($CuSO_4 \cdot 5H_2O$), zinc nitrate hexahydrate (Zn $(NO_3)2 \cdot 6H_2O$), 2-methylimidazole (HMIM), tetracycline (TC), tetracycline drug samples, methanol, and ultrapure water were produced in our laboratory, and all metal salts were purchased from Merck (Darmstadt, Germany).

Instrumentation

A Cary 60 Spectrophotometer (Agilent Technologies, USA) was used to obtain the UV–Vis absorption spectra. Fluorescence spectra were recorded via Cary Eclipse Fluorescence Spectrophotometer (Agilent Technologies, USA); both the emission and excitations slits were set at 5.0 nm. FTIR spectra were taken using Varian 640 FTIR spectrophotometer (Palo Alto, CA, USA). For the X-ray diffraction patterns (XRD spectra), Empyrean X-ray diffractometer was used to collect the X-ray diffraction patterns (PANalytical, Netherland). The scanning electron microscope (SEM) and transmission electron microscope (TEM) images are used to investigate the size of particles and to probe the extent of agglomeration of particles and their dispersion.

Synthesis of blue CuNCs

CuNCs were papered based on reports published in literature with modifications (Yang et al. 2014; Chattopadhyay 2014; Rajamanikandan and Ilanchelian 2018; Xiaoqing et al. 2015a). In a typical experiment, 25 mg of thiamine hydrochloride was dissolved in 20 mL ultrapure deionized water and then 4 mL of $CuSO_4.5H_2O$ (20 µM) added to the above solution. After the solution was stirred at room temperature for 5 min, the acidity of the solution was adjusted to pH 12 using 1.0 M NaOH until the color of solution changes from white hydrogel to purple. The mixture was reduced by quickly adding 3.0 mL of 1.0 M $NaBH_4$, and then the solution was stirred for 1 h at 55 °C. Finally, a brown solution was produced and shows blue emission under UV irradiation.

Synthesis of CuNCs@ZiF-8

Nanocomposite of CuNCs@ZiF-8 was prepared according to the previous work with some modification (Son et al. 2020). In brief, imidazole-CuNCs solution was prepared by dissolving 0.6 gm of 2-methylimidazole in 15 mL methanol. Then 2.5 mL CuNCs solution was added. Zinc ions solution was prepared by dissolving 0.2 gm of $Zn(NO_3)_2.6H_2O$ in 15 mL methanol. Then both

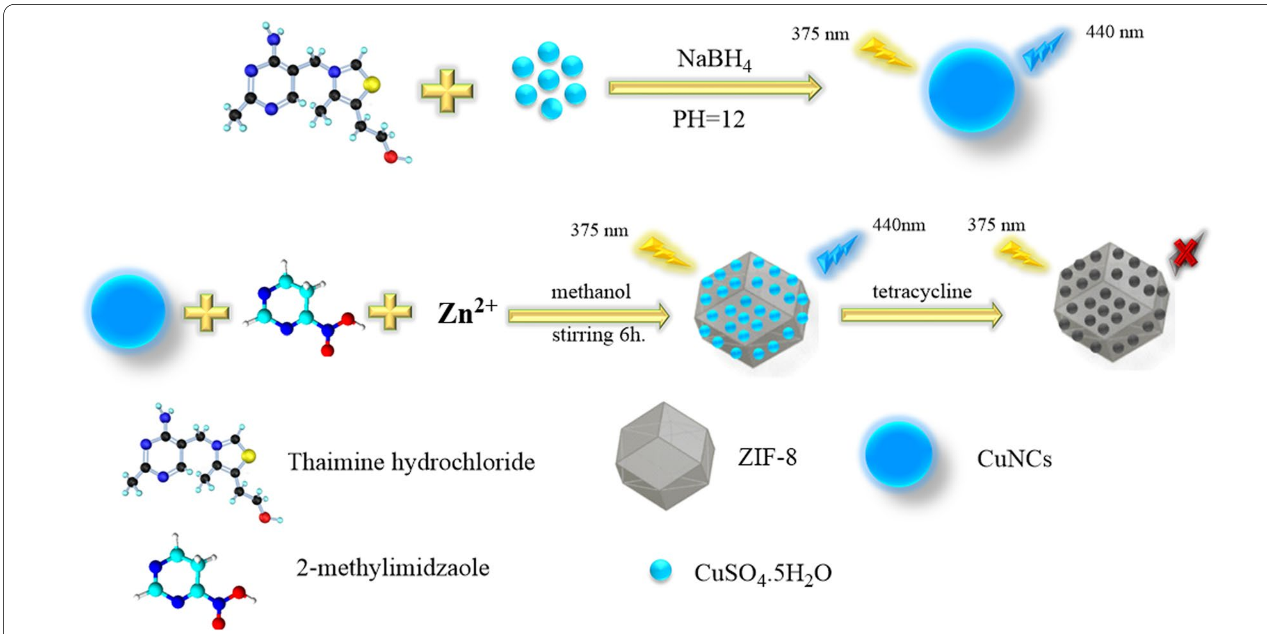

Fig. 1 Schematic presentation of preparation CuNCs@zif-8 for detection of tetracycline

imidazole-CuNCs and zinc ions solution were mixed and stirred for 6 h. The resultant CuNCs@ZIF-8 was separated and washed with methanol three times and finally dispersed in 40 ml methanol. The CuNCs@ZiF-8 is stable at least for 3 months.

Fluorescence assay of TC

In a typical assay, 20 µL of CuNCs@ZiF-8 dispersed in 5 mL of methanol, and then different concentrations of tetracycline were added to the mixture. After equilibrium for 5 min at room temperature, the fluorescence spectra were recorded at 440 nm with an excitation wavelength of 375 nm.

Drug sample preparation

Drug samples of tetracycline capsules were purchased from drug store. A 2.0 mL aliquot of each drug sample was spiked by adding appropriate amounts of standard tetracycline solution. The mixture was diluted to 3 times using methanol and analyzed by CuNCs@ZIF-8 probe.

Results and discussion

Synthesis and characterization of CuNCs@ZIF-8

Blue-emitting CuNCs were synthesized via a fast reduction process using thiamine hydrochloride as a template and stabilizing agent. To the best of our knowledge, it is the first-time thiamine hydrochloride is used in the preparation of nanoclusters. At the excitation wavelength of 375 nm, the as prepared CuNCs display blue fluorescence at 440 nm (Fig. 2A). It is known that ZIF-8 alone does not show any distinct fluorescence peak. Based on these results, it can be concluded that the fluorescence emission of CuNCs is well maintained after encapsulating in ZIF-8. The synthesized CuNCS@ZIF-8 was characterized by FTIR, TEM, SEM, and XRD.

In order to verify the reason of the fluorescence enhancement of CuNCs after encapsulation within the ZIF-8 structure and to investigate the contribution of the host–guest effects, we measured the fluorescence intensities of CuNCs@ZIF-8 nanostructure and CuNCs alone. As in Fig. 2A when CuNCs encapsulated in ZIF-8, the fluorescence intensity increases dramatically. The relative photoluminescence quantum yields (QYs) of CuNCs and CuNCs@ZIF-8 were determined to be 12.5% and 53.23%, respectively. The QY enhancement (about 5 times) in the CuNCs@ZIF-8 is attributed to the framework confinement and protection of MOF towards decreasing aggregation of CuNCs. Additionally, to confirm the enhancement is due to the confinement in the ZIF pores rather than to be from the effect of precursors, we mixed CuNCs with both 2-methylimidazole (ligand) and Zn^{2+} (metal) separately and together. Both solutions showed no effect in the enhancement of intensity CuNCs which rules out to be the enhancement due to the precursors, in opposite, it is exclusively due to the insertion of the clusters in the ZIF-8 pores. Figure 2B shows UV–Vis spectra of CuNCs and CuNCs@ZIF-8, the absorption peak of CuNCs and CuNCs@ZIF-8 at 364 nm.

The morphology and size of CuNCs, ZIF-8, and CuNCs@ZIF-8 were characterized by TEM and FE-SEM. As shown in Fig. 3a, the CuNCs display a spherical and road-like shape with average diameter were about 8–10 nm. TEM image (Fig. 3b) illustrates that the ZIF-8 nanostructure has the spherical shape and the average diameter was about 35–45 nm. Figure 3c, d shows that the particle sizes of CuNCs@ZIF-8 are in the range of

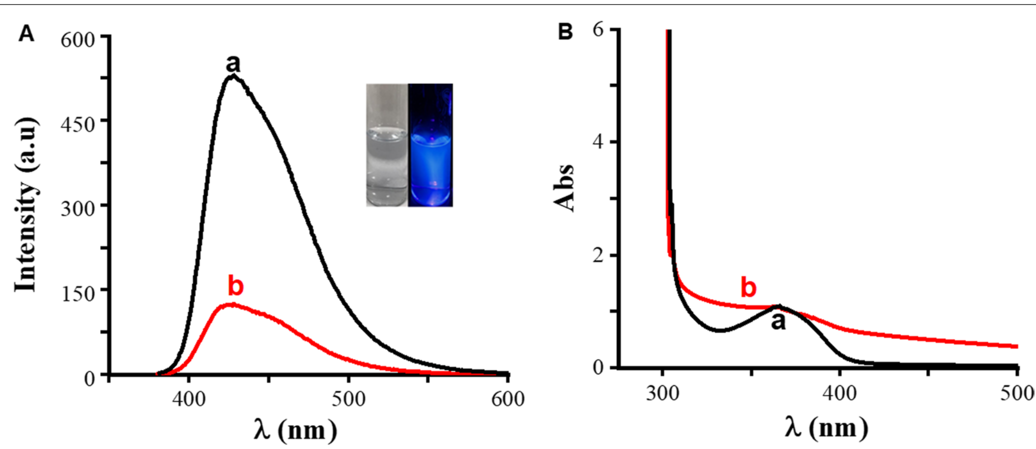

Fig. 2 **A** Fluorescence emission spectra of (a) CuNCs@ZIF-8, (b) CuNCs alone. The inset image shows the digital photographs of (right) pure CuNCs@ZIF-8, (left) CuNCs@ZIF-8 under ultraviolet light of 365 nm. **B** Absorption spectra of (a) CuNCs@ZIF-8, (b) CuNCs both of them the absorption spectrum at 364 nm

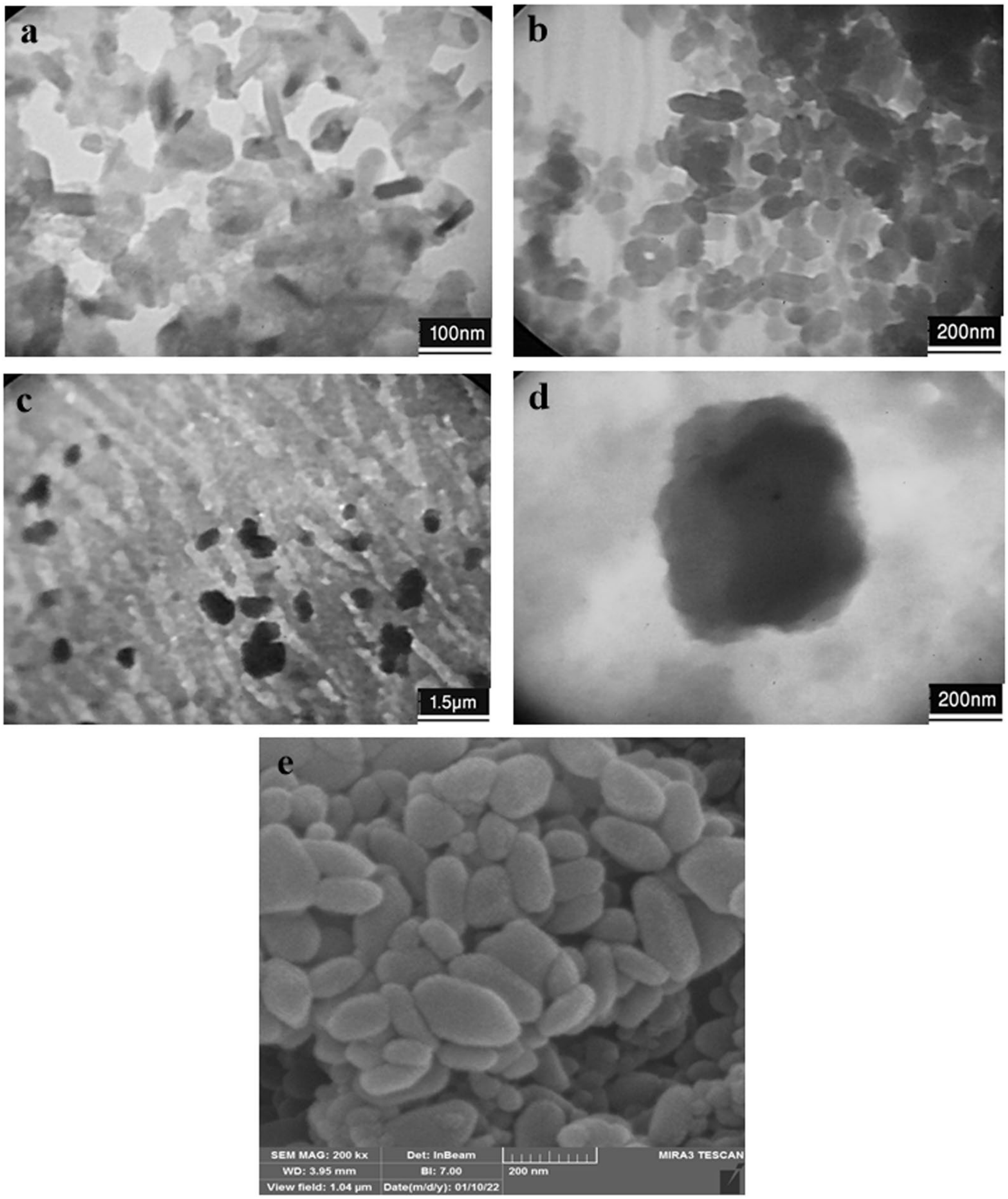

Fig. 3 **a** TEM image of CuNCs, **b** TEM image of ZIF-8, **c**–**d** TEM image of CuNCs@ZIF-8, **e** FE-SEM image of ZIF-8

200–300 nm. FE-SEM image as shown in Fig. 3e confirms that ZIF-8 nanostructures have monodisperse size distribution and the particle sizes are in the range of 30 and 50 nm.

The crystal structures of pure ZIF-8 and CuNCs@ZIF-8 were characterized by XRD. As shown in XRD patterns in Fig. 4A, pure ZIF-8 and CuNCs@ZIF-8 were conducted to verify that CuNCs encapsulation didn't influence the structure of ZIF-8. The reflection located in 2θ of 7.3 is attributed to a 1 peak, which was in accordance with the rhombic dodecahedron of the nanocrystals of ZIF-8 (Chen et al. 2018b), and the similar diffraction peaks in XRD of pure ZIF-8 and CuNCs@ZIF-8 were observed, which might due to the fact that there was no real interaction among CuNCs and ZIF-8 rather than just confinement of CuNCsiInto the ZIF-8 pores. The results indicated that the crystalline integrity of ZIF-8 was not affected after encapsulating CuNCs. Also, in the XRD spectra of CuNCs@ZIF-8 show that a reflection located 2θ of 60. Therefore, the diffraction peak of CuNCs not clearly observed due to the small size of CuNCs, the

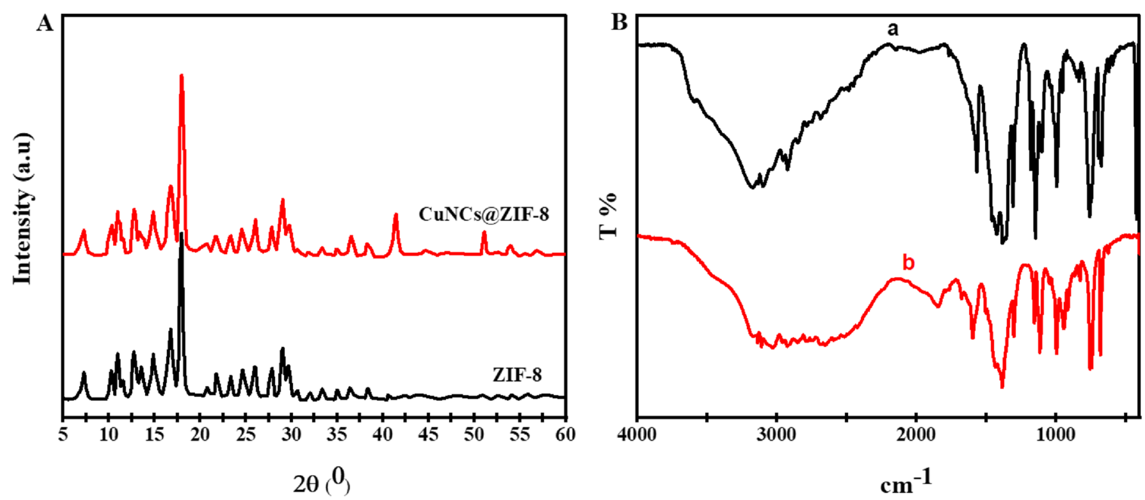

Fig. 4 **A** XRD patterns of the prepared ZIF-8 and CuNCs@ZIF-8; **B** (a) FTIR spectrum of ZIF-8 (black line) and (b) CuNCs@ZIF-8 (red line)

reflection located in 2θ of 42 and 50 crystals of Cu^0 based on (JCPDS 89–2838). (Wang et al. 2021a; Said et al. 2018)

FTIR spectra were also recorded for more structural characterization of ZIF-8, and CuNCsZIF-8. As exhibited in Fig. 4B, the spectrum of CuNCs@ZIF-8 was nearly same as that of ZIF-8. The FTIR spectra of ZIF-8 peaks between 2923 and 3170 cm^{-1} show the stretching mode of aliphatic and aromatic C–H of imidazole ring, respectively. FTIR absorption peaks for in-plane and out-of-plane bending of imidazole ring are at 692–758 and 952–1178 cm^{-1}, respectively. FTIR absorption peak at 421 cm^{-1} shows the stretching of Zn–N bond. (Malkar and Yadav 2018) Also, sharp peaks around 1307–1422 cm^{-1} exhibit the absorption band of C–N bond. The FTIR spectra of CuNCs@ZIF-8 cause to broad a peak at 3137–2653 cm^{-1} and disappearance peak Zn-N at 421 cm^{-1} (Hu, et al. 2020).

Analytical performance

The fluorescence emission of nanocomposite of CuNCs@ZIF-8 was quenched after addition of TC. Then, one can design a fluorescence probe for detection of TC in pharmaceutical formulations. To increase the sensitivity and selectivity for TC detection, pH was optimized. The effect of pH value on the intensity CuNCs@ZIF-8 was investigated in the pH range of 2.0–10.0. As shown in Fig. 5A, maximum fluorescence intensity was between pH 4 and 10. Therefore, pH 7.5, same as physiological pH, was selected for further measurements. Decreasing pH values induces the aggregation of CuNCs, leading to a color change and fluorescence quenching of the CuNCs (Xiaoqing et al. 2015b).

As show in Fig. 5B, the fluorescence intensity of the CuNCs@ZIF-8 at 440 nm gradually decreased upon the addition of TC. The fluorescence intensities are proportional to concentration of TC. Figure 5C shows the selectivity study, as CuNCs@ZIF-8 is highly selective for detection tetracycline among common pharmaceutical ingredients. The fluorescence intensity ratio (Fo/F) is linear as a function of the TC concentration in the range of 1–10 μM (Fig. 5D). The obtained linear equation ($y = 0.0399x + 1.0916$, $R^2 = 0.997$) was used for the quantification of TC. The LOD was calculated to be 0.30 μM (3S/N) and the relative standard deviation (RSD) for 10 measurements was 0.01%.

Determination of TC in drug samples

To investigate the applicability of the proposed method, our CuNCs encapsulating into ZIF-8 was used to detect TC concentration in pharmaceutical formulations. to calculate the spike recoveries and accuracy of our probe, a sample solution was spiked with different concentrations of 2, 3, and 4 μM of standard TC solutions. As shown in Table 1, the obtained results showed satisfactory recovery (recoveries ranging from 81.02% to 101.65%). Based on the data, the proposed CuNCs@ZIF-8 probe can be used in drug sample analysis.

Table 2 shows a comparison for the reported methods in literature with our proposed probe. As shown in the table, our nanocomposite has reliable LOD and linearity range.

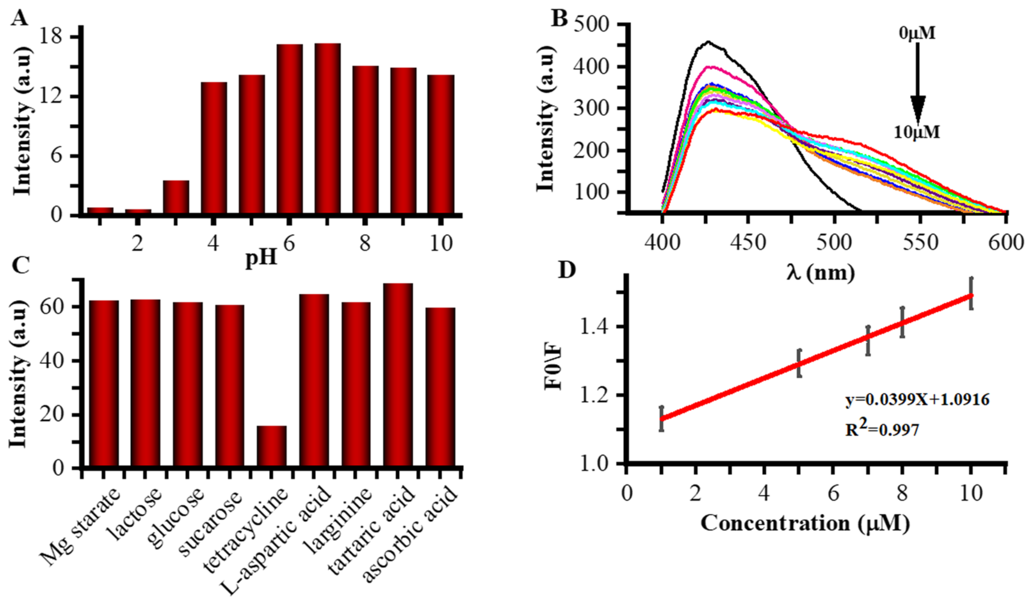

Fig. 5 **A** Fluorescence spectra of CuNCs@ZIF-8 probe in various pHs. **B** Fluorescence spectra of CuNCs@ZIF-8 probe upon the exposure of various concentrations of TC, **C** selectivity test for CuNCs@ZIF-8. **D** Calibration regression curve (The experimental conditions were λ_{ex} = 375 nm, pH = 7 and incubation times = 5 min)

Table 1 Results for the determination of TC in drug tablet

Sample	TC detection (μM)	Added (μM)	Found (μM)	Recovery %	RSD %
Tablet	3.29	2	5.301	101.65	3.283
		3	6.143	95.83	3.185
		4	6.508	81.03	2.677

Conclusions

In brief, we prepared stable and highly fluorescent CuNCs using thiamine hydrochloride as a template and stabilizing agent. To the best of our knowledge, it is for the first-time thiamine hydrochloride is used in the synthesis of CuNCs. The fluorescent emission was further enhanced (about five times) after *in situ* encapsulation of CuNCs into the framework of ZIF-8. The blue emission of CuNCs@ZIF-8 was quenched after addition of tetracycline. Chemical sensor based on CuNCs@ZIF-8 showed wide linearity and LOD as small as 0.97 μM for TC detection. The probe was used successfully for detecting TC in drug. Satisfactory accuracy and precision were calculated in addition to stability of the probe and easy operations. This approach is promising for real application as it has some advantages including simple, rapid, stable, and easy operation, thus holding a great potential for broad applications.

Table 2 Comparison of different fluorescent methods for TC sensing

Probe	Real sample	LOD	Linear range	Ref.
AuCuNCs@ZIF-8	Milk	4.8 nM	20–600 nM	Khataee et al. (2020)
Zr-MOF	Water	30 nM	–	Zhou et al. (2018)
MIL-53(Fe)\GCE	Water	0.026 μM	0.0643–1.53 μM	Chen et al. 2021)]
CuNCs	Milk and urine	40 nM	200 nM to 50 μM	Wang et al. (2021b)
AuNPs	Water	0.071 μM	0.10 to 5.00 μM	Qi et al. (2018)
AgNCs	Milk	0.47 μM	1.12 to 230 μM	Zhang et al. 2021)
CdTe-MIP	Drug	8.8 μM	70 μM–2.2 mM	Chen (2017)
CuNCs@ZIF-8	Drug	0.3 μM	1.0–10.0 μM	The present work

Acknowledgements
Authors thank the Department of Chemistry, College of Science, University of Sulaimani, for the opportunity to conduct this research. SH.M. Pirot thanks Aso Q. Hassan for his valuable help throughout this work.

Author contributions
SP conduct the experimental work,data analysis, and wrote the first draft. KMO supervised the whole research project, edited the draft, and prepared the manuscript. All authors read and approved the final manuscript.

Funding
The authors declare that there is no any funding, national or international grant, for this project. It is just conducted in the Department of Chemistry, University of Sulaimani.

Availability of data and materials
All the data are available based on request.

Declarations

Competing interests
The authors declare that they have no known competing financial interests or personal relationships that could have appeared to influence the work reported in this paper.

Received: 9 April 2022 Accepted: 20 June 2022
Published online: 27 June 2022

References

Aga DS, et al. Determination of the persistence of tetracycline antibiotics and their degradates in manure-amended soil using enzyme-linked immunosorbent assay and liquid chromatography-mass spectrometry. J Agric Food Chem. 2005;53:7165–71.
Allendorf MD, Bauer CA, Bhakta RK, Houk RJT. Luminescent metal–organic frameworks. Chem Soc Rev. 2009;38:1330–52.
Bågenholm R, Hagberg H, Kjellmer I. Impact of reoxygenation with oxygen and air on the extent of the brain damage after hypoxia-ischaemia in neonatal rats. Acta Paediatr Int J Paediatr. 1996;85:1228–31.
Baumann AE, Burns DA, Liu B, Thoi VS. Metal–organic framework functionalization and design strategies for advanced electrochemical energy storage devices. Commun Chem. 2019;2:1–14.
Bazargan M, Ghaemi F, Amiri A, Mirzaei M. Metal–organic framework-based sorbents in analytical sample preparation. Coord Chem Rev. 2021;445:214107.
Ben-Amram Y, Riskin M, Willner I. Selective and enantioselective analysis of mono- and disaccharides using surface plasmon resonance spectroscopy and imprinted boronic acid-functionalized Au nanoparticle composites. Analyst. 2010;135:2952–9.
Bin Q, Wang M, Wang L. Ag nanoparticles decorated into metal–organic framework (Ag NPs/ZIF-8) for electrochemical sensing of chloride ion. Nanotechnology. 2020;31:125601–09.
Buso D, et al. Highly luminescent metal–organic frameworks through quantum dot doping. Small. 2012;8:80–8.
Chandra R, Nath M. Controlled synthesis of AgNPs@ZIF-8 composite: Efficient heterogeneous photocatalyst for degradation of methylene blue and congo red. J Water Process Eng. 2020;36:101266.
Ghosh R, Sahoo AK, Ghosh SS, Paul A, Chattopadhyay A. Blue-emitting copper nanoclusters synthesized in the presence of lysozyme as candidates for cell labeling. ACS Appl Mater Interfaces. 2014;6(6):3822–3828.
Chen JL. Determination of tetracycline using imprinted polymethacrylates along with fluorescent CdTe quantum dots on plastic substrates. Microchim Acta. 2017;184:1335–43.
Chen L, Luque R, Li Y. Controllable design of tunable nanostructures inside metal–organic frameworks. Chem Soc Rev. 2017a;46:4614–30.
Chen T, et al. Crystallization-induced emission enhancement: a novel fluorescent Au–Ag bimetallic nanocluster with precise atomic structure. Sci Adv. 2017b;3:1–8.
Chen L, Luque R, Li Y. Encapsulation of metal nanostructures into metal–organic frameworks. Dalt Trans. 2018a;47:3663–8.
Chen TT, Yi JT, Zhao YY, Chu X. Biomineralized metal–organic framework nanoparticles enable intracellular delivery and endo-lysosomal release of native active proteins. J Am Chem Soc. 2018b;140:9912–20.
Ameen SSM, Mohammed NMS, Omer KM. Visual monitoring of silver ions and cysteine using bi-ligand Eu-based metal organic framework as a reference signal: Color tonality. Microchem J. 2022;181:107721.
Chin M, et al. Rhodamine B degradation by nanosized zeolitic imidazolate framework-8 (ZIF-8). RSC Adv. 2018;8:26987–97.
Chopra I, Roberts M. Tetracycline Antibiotics: mode of action, applications, molecular biology, and epidemiology of bacterial resistance. Microbiol Mol Biol Rev. 2001;65:232–60.
Conzuelo F, Gamella M, Campuzano S, Reviejo AJ, Pingarrón JM. Disposable amperometric magneto-immunosensor for direct detection of tetracyclines antibiotics residues in milk. Anal Chim Acta. 2012;737:29–36.
Cui Y, Yue Y, Qian G, Chen B. Luminescent functional metal–organic frameworks. Chem Rev. 2012;112:1126–62.
Cui Y, et al. Metal–organic Frameworks as Platforms for Functional Materials. Acc Chem Res. 2016;49:483–93.
Doonan C, Riccò R, Liang K, Bradshaw D, Falcaro P. Metal–organic frameworks at the biointerface: synthetic strategies and applications. Acc Chem Res. 2017;50:1423–32.
Düren T, Snurr RQ. Assessment of isoreticular metal–organic frameworks for adsorption separations: a molecular simulation study of methane/n-butane mixtures. J Phys Chem B. 2004;108:15703–8.
Fahelelbom KMS. Analysis of certain tetracyclines and oxytetracyclines through charge transfer complexation. Am J Pharmacol Toxicol. 2008;3:212–8.
Gao C, et al. Rational design microporous pillared-layer frameworks: syntheses, structures and gas sorption properties. CrystEngComm. 2009;11:177–82.
Ghaee A, Karimi M, Lotfi-Sarvestani M, Sadatnia B, Hoseinpour V. Preparation of hydrophilic polycaprolactone/modified ZIF-8 nanofibers as a wound dressing using hydrophilic surface modifying macromolecules. Mater Sci Eng C. 2019;103:109767–770.
Han H, He Z. Chemiluminescence determination of tetracyclines using a permanganate system. Anal Sci. 1999;15(5):467–70.
Han X, et al. Controlled synthesis of concave cuboctahedral nitrogen-rich metal–organic framework nanoparticles showing enhanced catalytic activation of epoxides with carbon dioxide. CrystEngComm. 2015;17:8596–601.
Han TT, Yang J, Liu YY, Ma JF. Rhodamine 6G loaded zeolitic imidazolate framework-8 (ZIF-8) nanocomposites for highly selective luminescent sensing of Fe^{3+}, Cr^{6+} and aniline. Microporous Mesoporous Mater. 2016;228:275–88.
Hao J, et al. Ratiometric fluorescent detection of Cu^{2+} with carbon dots chelated Eu-based metal–organic frameworks. Sensors Actuators B Chem. 2017;245:641–7.
Hoseinpour V, Shariatinia Z. Applications of zeolitic imidazolate framework-8 (ZIF-8) in bone tissue engineering: a review. Tissue Cell. 2021;72:101588.
Hu Y, Kazemian H, Rohani S, Huang Y, Song Y. In situ high pressure study of ZIF-8 by FTIR spectroscopy. Chem Commun. 2011;47:12694–6.
Hu M, et al. In-situ fabrication of ZIF-8 decorated layered double oxides for adsorption and photocatalytic degradation of methylene blue. Microporous Mesoporous Mater. 2018a;271:68–72.
Hu X, Liu X, Zhang X, Chai H, Huang Y. One-pot synthesis of the CuNCs/ZIF-8 nanocomposites for sensitively detecting H_2O_2 and screening of oxidase activity. Biosens Bioelectron. 2018b;105:65–70.
Hu X, et al. A molecularly imprinted fluorescence nanosensor based on upconversion metal–organic frameworks for alpha-cypermethrin specific recognition. Microchim Acta. 2020;187:632. https://doi.org/10.1007/s00604-020-04610-2.
Jalili R, Khataee A, Rashidi MR, Luque R. Dual-colored carbon dot encapsulated metal–organic framework for ratiometric detection of glutathione. Sensors Actuators B Chem. 2019;297:126775.
Jeon M, Kim J, Paeng KJ, Park SW, Paeng IR. Biotin-avidin mediated competitive enzyme-linked immunosorbent assay to detect residues of tetracyclines in milk. Microchem J. 2008;88:26–31.
Jing HP, Wang CC, Zhang YW, Wang P, Li R. Photocatalytic degradation of methylene blue in ZIF-8. RSC Adv. 2014;4:54454–62.

Khataee A, Jalili R, Dastborhan M, Karimi A, Ebadi Fard Azar A. Ratiometric visual detection of tetracycline residues in milk by framework-enhanced fluorescence of gold and copper nanoclusters. Spectrochim Acta Part A Mol Biomol Spectrosc. 2020;242:118715.

Kolmykov O, et al. Microfluidic reactors for the size-controlled synthesis of ZIF-8 crystals in aqueous phase. Mater Des. 2017;122:31–41.

Koo W-T, Jang J-S, Kim I-D. Metal–organic Frameworks for Chemiresistive Sensors. Chem. 2019;5:1938–63.

Kreno LE, et al. Metal–organic framework materials as chemical sensors. Chem Rev. 2012;112:1105–25.

Kumar P, Deep A, Kim KH. Metal organic frameworks for sensing applications. TrAC Trends Anal Chem. 2015;73:39–53.

Lai Z. Development of ZIF-8 membranes: opportunities and challenges for commercial applications. Curr Opin Chem Eng. 2018;20:78–85.

Lee YR, et al. ZIF-8: a comparison of synthesis methods. Chem Eng J. 2015;271:276–80.

Lewis DW, et al. Zeolitic imidazole frameworks: structural and energetics trends compared with their zeolite analogues. CrystEngComm. 2009;11:2272–6.

Li H, Eddaoudi M, O'Keeffe M, Yaghi OM. Design and synthesis of an exceptionally stable and highly. Nature. 1999;402:276–9.

Li JR, Kuppler RJ, Zhou HC. Selective gas adsorption and separation in metal–organic frameworks. Chem Soc Rev. 2009;38:1477–504.

Li H, et al. An integrated nanocatalyst combining enzymatic and metal–organic framework catalysts for cascade degradation of organophosphate nerve agents. Chem Commun. 2018a;54:10754–7.

Li G, Wang X, Zhang J. Carbon dots for promoting the growth of ZIF-8 crystals to obtain fluorescent powders and their application for latent fingerprint imaging. CrystEngComm. 2018b;20:5056–60.

Lin YS, Lin YF, Nain A, Huang YF, Chang HT. A critical review of copper nanoclusters for monitoring of water quality. Sensors Actuators Rep. 2021;3:100026.

Liu Y, Kasik A, Linneen N, Liu J, Lin YS. Adsorption and diffusion of carbon dioxide on ZIF-68. Chem Eng Sci. 2014;118:32–40.

Liu R, Yu T, Shi Z, Wang Z. The preparation of metal–organic frameworks and their biomedical application. Int J Nanomed. 2016;11:1187–200.

Liu N, Hao J, Chen L, Song Y, Wang L. Ratiometric fluorescent detection of Cu^{2+} based on dual-emission ZIF-8@rhodamine-B nanocomposites. Luminescence. 2019;34:193–9.

Majewski MB, et al. Enzyme encapsulation in metal–organic frameworks for applications in catalysis. CrystEngComm. 2017;19:4082–91.

Malkar RS, Yadav GD. Synthesis of cinnamyl benzoate over novel heteropoly acid encapsulated ZIF-8. Appl Catal A Gen. 2018;560:54–65.

Mohammed LJ, Omer KM. Dual functional highly luminescence B, N Co-doped carbon nanodots as nanothermometer and Fe^{3+}/Fe^{2+} sensor. Sci Rep. 2020;10:3028.

Müller-Buschbaum K, Beuerle F, Feldmann C. MOF based luminescence tuning and chemical/physical sensing. Microporous Mesoporous Mater. 2015;216:171–99.

Ni Y, Li S, Kokot S. Simultaneous voltammetric analysis of tetracycline antibiotics in foods. Food Chem. 2011;124:1157–63.

Noh K, Lee J, Kim J. Compositions and structures of zeolitic imidazolate frameworks. Isr J Chem. 2018;58:1075–88.

Omer KM, Idrees SA, Hassan AQ, Jamil LA. Amphiphilic fluorescent carbon nanodots as a selective nanoprobe for nitrite and tetracycline both in aqueous and organic solutions. New J Chem. 2020;44:5120–6.

Omer KM, Hassan AQ. Chelation-enhanced fluorescence of phosphorus doped carbon nanodots for multi-ion detection. Microchim Acta. 2017;184:2063–2071.

Omer KM, Sartin M. Dual-mode colorimetric and fluorometric probe for ferric ion detection using N-doped carbon dots prepared via hydrothermal synthesis followed by microwave irradiation. Opt Mater (Amst). 2019;94:330–336.

Omer KM, Hama Aziz KH, Mohammed SJ. Improvement of selectivity: via the surface modification of carbon nanodots towards the quantitative detection of mercury ions. New J Chem. 2019;43:12979–12986.

Online VA, Nallagondu CGR, Kumar SD. RSC advances. RSC Adv. 2014;4:17196–205.

Park KS, et al. ZIFs—first synthesis. Proc Natl Acad Sci. 2006;103:10186–91.

Qi M, et al. A simple colorimetric analytical assay using gold nanoparticles for specific detection of tetracycline in environmental water samples. Anal Methods. 2018;10:3402–7.

Qu ZG, Wang H, Zhang W. Highly efficient adsorbent design using a Cu-BTC/CuO/carbon fiber paper composite for high CH4/N2 selectivity. RSC Adv. 2017;7:14206–18.

Rajamanikandan R, Ilanchelian M. Protein-protected red emittive copper nanoclusters as a fluorometric probe for highly sensitive biosensing of creatinine. Anal Methods. 2018;10:3666–74.

Rowsell JLC, Spencer EC, Eckert J, Howard JAK, Yaghi OM. Chemistry: gas adsorption sites in a large-pore metal–organic framework. Science (80-). 2005;309:1350–4.

Said K, Qamhieh N, Awwad F, Ayesh AI. Fabrication and characterization of size-selected Cu nanoclusters using a magnetron sputtering source. Sensors Actuators A Phys. 2018;277:112–6.

Sarmah AK, Meyer MT, Boxall ABA. A global perspective on the use, sales, exposure pathways, occurrence, fate and effects of veterinary antibiotics (VAs) in the environment. Chemosphere. 2006;65:725–59.

Shah M, McCarthy MC, Sachdeva S, Lee AK, Jeong HK. Current status of metal–organic framework membranes for gas separations: promises and challenges. Ind Eng Chem Res. 2012;51:2179–99.

Shahat A, Hassan HMA, Azzazy HME. Optical metal–organic framework sensor for selective discrimination of some toxic metal ions in water. Anal Chim Acta. 2013;793:90–8.

Shen L, Chen J, Li N, He P, Li Z. Rapid colorimetric sensing of tetracycline antibiotics with in situ growth of gold nanoparticles. Anal Chim Acta. 2014;839:83–90.

So MC, Wiederrecht GP, Mondloch JE, Hupp JT, Farha OK. Metal–organic framework materials for light-harvesting and energy transfer. Chem Commun. 2015;51:3501–10.

Son YR, Kwak M, Lee S, Kim HS. Strategy for encapsulation of CdS quantum dots into zeolitic imidazole frameworks for photocatalytic activity. Nanomaterials. 2020;10:1–9.

Spisso BF, de Oliveira e Jesus AL, de Araújo Júnior MAG, Monteiro MA. Validation of a high-performance liquid chromatographic method with fluorescence detection for the simultaneous determination of tetracyclines residues in bovine milk. Anal Chim Acta. 2007;581:108–17.

Sun K, et al. Functionalization of mixed ligand metal–organic frameworks as the transport vehicles for drugs. J Colloid Interface Sci. 2017a;486:128–35.

Sun X, Gao G, Yan D, Feng C. Synthesis and electrochemical properties of Fe_3O_4@MOF core-shell microspheres as an anode for lithium ion battery application. Appl Surf Sci. 2017b;405:52–9.

Sutrisna PD, Prasetya N, Himma NF, Wenten IG. A mini-review and recent outlooks on the synthesis and applications of zeolite imidazolate framework-8 (ZIF-8) membranes on polymeric substrate. J Chem Technol Biotechnol. 2020;95:2767–74.

Taheri M, et al. Stability of ZIF-8 nanopowders in bacterial culture media and its implication for antibacterial properties. Chem Eng J. 2021;413:127511.

Tian R, et al. Localization of Au nanoclusters on layered double hydroxides nanosheets: confinement-induced emission enhancement and temperature-responsive luminescence. Adv Funct Mater. 2015;25:5006–15.

Troyano J, Carné-Sánchez A, Avci C, Imaz I, Maspoch D. Colloidal metal–organic framework particles: the pioneering case of ZIF-8. Chem Soc Rev. 2019;48:5534–46.

Wan X, et al. Programmed release of dihydroartemisinin for synergistic cancer therapy using a CaCO3 mineralized metal–organic framework. Angew Chemie Int Ed. 2019;58:14134–9.

Wang LF, Peng JD, Liu LM. A reversed-phase high performance liquid chromatography coupled with resonance Rayleigh scattering detection for the determination of four tetracycline antibiotics. Anal Chim Acta. 2008;630:101–6.

Wang H, Zhu QL, Zou R, Xu Q. Metal–organic frameworks for energy applications. Chem. 2017a;2:52–80.

Wang X, et al. Nanocapsules engineered from polyhedral ZIF-8 templates for bone-targeted hydrophobic drug delivery. Biomater Sci. 2017b;5:658–62.

Wang Z, Chen B, Rogach AL. Synthesis, optical properties and applications of light-emitting copper nanoclusters. Nanoscale Horizons. 2017c;2:135–46.
Wang Z, Yu G, Xia J, Zhang F, Liu Q. One-step synthesis of a Methylene Blue@ZIF-8-reduced graphene oxide nanocomposite and its application to electrochemical sensing of rutin. Microchim Acta. 2018;185:1–8.
Wang F, Zheng T, Xiong R, Wang P, Ma J. CDs@ZIF-8 modified thin film polyamide nanocomposite membrane for simultaneous enhancement of chlorine-resistance and disinfection byproducts removal in drinking water. ACS Appl Mater Interfaces. 2019;11:33033–42.
Wang Y, et al. Facile synthesis of CDs@ZIF-8 nanocomposites as excellent peroxidase mimics for colorimetric detection of H_2O_2 and glutathione. Sensors Actuators B Chem. 2021;329:129115.
Wang C, et al. Dual-emission fluorescence sensor based on biocompatible bovine serum albumin stabilized copper nanoclusters for ratio and visualization detection of hydrogen peroxide. Dye Pigment. 2021a;190: 109312.
Wang HB, Tao BB, Mao AL, Xiao ZL, Liu YM. Self-assembled copper nanoclusters structure-dependent fluorescent enhancement for sensitive determination of tetracyclines by the restriction intramolecular motion. Sensors Actuators B Chem. 2021b;348: 130729.
Wei X, Wang Y, Huang Y, Fan C. Composite ZIF-8 with CQDs for boosting visible-light-driven photocatalytic removal of NO. J Alloys Compd. 2019;802:467–76.
Wei YS, Zhang M, Zou R, Xu Q. Metal–organic framework-based catalysts with single metal sites. Chem Rev. 2020;120:12089–174.
Wu X, Xiong S, Mao Z, Hu S, Long X. A designed ZnO@ZIF-8 core-shell nanorod film as a gas sensor with excellent selectivity for H2 over CO. Chem A Eur J. 2017;23:7969–75.
Xiaoqing L, et al. Fast synthesis of copper nanoclusters through the use of hydrogen peroxide additive and their. New J Chem. 2015a. https://doi.org/10.1039/C5NJ00831J.
Xiaoqing L, Ruiyi L, Xiaohuan L, Zaijun L. Ultra sensitive and wide-range pH sensor based on the BSA-capped Cu nanoclusters fabricated by fast synthesis through the use of hydrogen peroxide additive. RSC Adv. 2015b;5:48835–41.
Yaghi OM, Li G, Li H. Yaghi-selective binding and removal of guests in a imcroporous metal–organic framework. Nature. 1995;378:703–6.
Yaghi OM, et al. Reticular synthesis and the design of new materials. Nature. 2003;423:705–14.
Yang X, et al. One-step synthesis and applications of fluorescent Cu nanoclusters stabilized by l-cysteine in aqueous solution. Anal Chim Acta. 2014;847:49–54.
Zhang CF, et al. A novel magnetic recyclable photocatalyst based on a core-shell metal–organic framework Fe3O4@MIL-100(Fe) for the decolorization of methylene blue dye. J Mater Chem A. 2013;1:14329–34.
Zhang Y, et al. Luminescent sensors based on metal–organic frameworks. Coord Chem Rev. 2018;354:28–45.
Zhang Y, et al. The synthesis of high bright silver nanoclusters with aggregation-induced emission for detection of tetracycline. Sensors Actuators B Chem. 2021;326:129009.
Zhou Y, et al. Detection and removal of antibiotic tetracycline in water with a highly stable luminescent MOF. Sensors Actuators B Chem. 2018;262:137–43.

Publisher's Note